

Evaluation and Projection of Vb-Cyclones and Associated North-Western Mediterranean Sea State in Regional Coupled Climate Simulations

Praveen Kumar Pothapakula (✉ pothapakula@iau.uni-frankfurt.de)

Goethe-Universität Frankfurt am Main <https://orcid.org/0000-0002-5654-7975>

Amelie Hoff

Deutscher Wetterdienst

Anika Obermann Hellhund

Goethe-Universität Frankfurt am Main

Timo Keber

Goethe-Universität Frankfurt am Main: Goethe-Universität Frankfurt am Main

Bodo Ahrens

Goethe-Universität Frankfurt am Main

Research Article

Keywords: Regional Coupled Climate Modeling, Vb-Cyclones, Precipitation, Air-Sea Interactions

Posted Date: December 8th, 2021

DOI: <https://doi.org/10.21203/rs.3.rs-1139190/v1>

License:   This work is licensed under a Creative Commons Attribution 4.0 International License.

[Read Full License](#)

1 **Evaluation and projection of Vb-cyclones and**
2 **associated North-Western Mediterranean Sea state**
3 **in regional coupled climate simulations**

4 **Praveen Kumar Pothapakula¹ · Amelie**
5 **Hoff^{1,2} · Anika Obermann-Hellhund¹ ·**
6 **Timo Keber¹ · Bodo Ahrens¹**

7
8 Received: date / Accepted: date

9 **Abstract** Vb-cyclones propagating from the North-Western Mediterranean
10 Sea into Central Europe are often associated with extreme precipitation. This
11 study explores the state & process chains linking the North-Western Mediter-
12 ranean Sea and the Vb-event precipitation in Danube, Elbe, and Odra catch-
13 ments in regional coupled atmosphere-ocean climate simulations with COSMO-
14 CLM+NEMO. Two high-resolution simulations, an evaluation simulation (1951-
15 2005) downscaling the centennial ERA-20C reanalysis and a continuous simu-
16 lation (historical 1951-2005 + RCP-8.5 future scenario 2006-2099) downscaling
17 the EC-EARTH global climate RCP-8.5 projection are used for this purpose.
18 Sea surface temperature (SST) validation with observations over the Mediter-
19 ranean Sea reveals a cold bias ($\approx 1 - 1.5$ K) in the historical & evaluation
20 simulations. There is a good agreement in mean annual Vb-cyclone frequency
21 between the evaluation (9.7 events/year) and the historical (10.1 events/year)
22 simulations. But, there are significant discrepancies in the seasonal cycle. The
23 mean cyclone intensity measured with minimum central pressure, track den-
24 sity, and precipitation rankings in the catchments also show good agreement.
25 A basin-average SST warming of $\approx 2.5 - 3$ K, but insignificant changes in Vb-
26 frequency, mean intensity, and precipitation in the catchments are projected
27 by the end of the 21st century. The North-Western Mediterranean SST, evapo-
28 ration, and wind speed anomalies corresponding to the precipitation rankings
29 over the three catchments & associated process chains differ between the evalu-
30 ation & historical simulations. In the evaluation simulation, Vb-cyclone precip-
31 itation rankings correspond with SST, evaporation, and wind speed anomalies,
32 while in the historical & the future simulation no such correspondence is seen.
33 Especially the Adriatic & Ionian basins show no sensitivity to the Vb events
34 in the EC-EARTH driven simulation. The change in the processes might be

¹ Institute for Atmospheric and Environmental Sciences, Goethe University Frankfurt am
Main, Altenhöferallee 1, 60438 Frankfurt am Main, Germany.

² now at Deutscher Wetterdienst, Offenbach, Germany

35 because of the emergence of simulation biases inherited from the driving EC-
36 EARTH global simulation.

37 **Keywords** Regional Coupled Climate Modeling; · Vb-Cyclones · Precipitation · Air-Sea Interactions
38

39 1 Introduction

40 Observational and modeling studies relating to the global temperature and
41 precipitation changes provide confidence in the current ongoing global warming
42 (Stocker et al, 2013). Changes in the extreme weather and climate events
43 such as warm/cold days and nights, heat waves, droughts, heavy precipitation
44 events induced by the anthropogenic global warming were observed in the
45 last century (Fischer et al, 2013; Wilcox and Donner, 2007; Trenberth, 1999;
46 Nishant and Sherwood, 2021; Beniston et al, 2007; Seneviratne et al, 2012).
47 Specifically, short-term precipitation extremes often result in heavy damage
48 to infrastructure and life, and hence are in need of further investigations.

49 Over Central Europe, extra-tropical cyclones named Vb-cyclones are often
50 associated with extreme precipitation, especially in the summer season
51 (Hofstätter et al, 2018; Blöschl et al, 2013). These Vb-cyclones develop over
52 the North-Western Mediterranean Sea typically over the Gulf of Lions and
53 travel northeastward through the eastern Alps to Central Europe (van Beber,
54 1891; Messmer et al, 2015). Often, extreme precipitation occurring in the
55 catchments of Danube, Elbe and Odra is linked to the Vb-cyclones.

56 Though the occurrence of Vb-cyclones is rare (typically about 4-10 events
57 on average per year) they are of considerable importance due to the extreme
58 precipitation they bring to Central and Eastern Europe (Hofstätter et al, 2016;
59 Messmer et al, 2015). These events occur throughout the year with a peak frequency
60 in spring (Hofstätter et al, 2016, 2018). The Vb-events are typically fed
61 from the evaporation over continental land and nearby oceans. For example,
62 enhanced evaporation over the Mediterranean Sea and subsequent increase of
63 available total water content in the atmosphere during Vb-cyclones was studied
64 by Hofstätter and Chimani (2012) & Messmer et al (2017). Based on a
65 model sensitivity study, Volosciuk et al (2016) reported an increase in precipitation
66 by 17% over Central Europe with warmer sea surface temperatures (SST) over the
67 Mediterranean Sea compared with a simulation run by average Mediterranean SST
68 for the period 1970-1999. Results from Volosciuk et al (2016) relied on a stand-alone
69 coarse-resolution global atmosphere model without dynamic coupling of the ocean,
70 missing crucial air-sea feedback processes. The role of the Mediterranean Sea in
71 enhancing the August 2002 flood in the early stages was shown in Sodemann et al
72 (2009); James et al (2004); Gan-goiti et al (2011). Furthermore, a sensitivity study
73 by Messmer et al (2017) confirmed the Mediterranean Sea role in supplying moisture
74 to Vb-cyclones. However, other studies concluded that the moisture transport from the
75 North Atlantic, Black Sea, continental moisture are major sources contributing to
76

77 the precipitable water for Vb-cyclones (James et al, 2004; Gangoiti et al, 2011;
78 Krug et al, 2021a).

79 Krug et al (2021a) analyzed about 1107 Vb-cyclone events simulated by
80 a regional coupled climate model during the period 1901-2010. Their study
81 concluded that the North-Western Mediterranean Sea played an active role in
82 the early stage intensification of the Vb-cyclones and also in pre-moistening
83 the continental land. Furthermore, high precipitation Vb-cyclone events were
84 associated with anomalously high dynamically driven evaporation. However,
85 with Lagrangian moisture source diagnostics on selected 16 Vb-events, their
86 study revealed that continental moisture recycling, the North Sea, the Baltic
87 Sea, the North Atlantic, and the Black Sea were major sources of moisture
88 supply to the Vb-cyclones. Krug et al (2021b) reported a significant informa-
89 tion exchange between the evaporation over the North-Western Mediterranean
90 Sea and Vb-cyclone precipitation over the Odra catchment. Above mentioned
91 studies highlight the North-Western Mediterranean Sea's role.

92 Though the Vb-cyclone events and the role of the Mediterranean Sea as a
93 moisture source were investigated in the past studies, the Vb-cyclone's future
94 projections and the role played by the Mediterranean Sea in the warming cli-
95 mate are yet to be investigated. Especially, the Mediterranean Sea being a hot
96 spot of climate change, investigating its role in the future Vb-cyclones is of
97 extreme importance. Using a global climate model (GCM), ECHAM5/OM1,
98 Nissen et al (2013) reported a decrease in the number of Vb-cyclones by the end
99 of the 21st century but an increase in precipitation amount by 16% compared
100 to the present. Messmer et al (2020), investigated the climate change impacts
101 on Vb-cyclone characteristics using a global climate model, i.e., Community
102 Earth System Model (CESM) ensemble simulations. Their results confirmed
103 a minor decrease in the frequency of Vb-cyclones from 2.9 to 2.6 Vb-cyclones
104 per year by the end of 21st century. They also found a subtle eastward shift in
105 the Vb-cyclone frequency pattern. Furthermore, by downscaling the 10 heavi-
106 est precipitation Vb-cyclone events with the Weather Research and Forecast-
107 ing (WRF) model in future and historical periods, they reported insignificant
108 changes in the total precipitation amount. It is to be noted that the study
109 by Messmer et al (2020) downscaled only 10 Vb-cyclone heavy precipitation
110 events in the past and future periods.

111 To simulate mesoscale systems such as the Vb-cyclones and analyze their
112 climatic characteristics, high-resolution regional climate model simulations in
113 long centennial periods are desirable. Mittermeier et al (2019) using a Cana-
114 dian Regional Climate Model Large Ensemble (CRCM5-LE) (Leduc et al,
115 2019) at a resolution of about 12 km (0.11°) studied future Vb-cyclone fre-
116 quency and precipitation changes over Bavaria from 1950-2099. They reported
117 a non-significant increase in the absolute number of Vb-cyclones per year in
118 the future period. Also, a significant decrease in future summer Vb-cyclone
119 frequency and increase in spring. A significant increase in daily precipitation
120 intensity was also reported over Bavaria.

121 The Coordinated Regional Climate Downscaling Experiment (CORDEX)
122 is an initiative that coordinates scientific groups for such high-resolution re-

123 gional climate data sets (Giorgi, 2006). The regional climate model COSMO-
124 CLM is used for dynamically downscaling GCMs over various CORDEX do-
125 mains (Asharaf and Ahrens, 2015; Russo et al, 2020; Drobinski et al, 2020;
126 Evans et al, 2021). The added value of such high-resolution simulations was
127 well documented in the studies by Schlemmer et al (2018); Imamovic et al
128 (2019); Panosetti et al (2019); Hentgen et al (2019); Brogli et al (2019); Sørland
129 et al (2021). However, the COSMO-CLM often uses prescribed SSTs from the
130 driving GCMs which are handicapped by their coarse resolution and unrealistic
131 air-sea dynamic interactions. Especially given the importance of the Mediter-
132 ranean Sea in the evolution of Vb-cyclone events, a realistic and dynamically
133 interactive ocean model is thus important.

134 The COSMO-CLM is coupled to Nucleus for European Modeling of the
135 Ocean (NEMO) over the Mediterranean sea (NEMOMED12) along with a
136 river run-off model TRIP to make the regional system dynamically interactive
137 (Akhtar et al, 2018). The added value of such a coupled regional system was
138 reported by Kelemen et al (2019) on the representation of European continen-
139 tal precipitation. Furthermore, Primo et al (2019) reported the added value
140 in terms of extreme air temperatures. This coupled system was earlier used to
141 study Vb-cyclones in the historical period by Akhtar et al (2019) and Krug
142 et al (2021a). Their study demonstrated the ability of the coupled system in
143 representing the past Vb-cyclone events realistically. Furthermore, Krug et al
144 (2021a) analyzed the total precipitation sums of a few selected Vb-cyclone
145 events (1901–2010) simulated by the coupled system driven by the ERA-20C
146 reanalysis. They reported that the coupled system precipitation patterns &
147 magnitudes agree well with the CRU (Harris et al, 2020) and the E-OBS
148 (Cornes et al, 2018) precipitation observational data sets.

149 In the current study, we apply the regional climate coupled model (COSMO-
150 CLM–NEMOMED12–TRIP) for the period 1951–2099 continuously using the
151 EC-EARTH GCM as driving data. The simulation used historical greenhouse
152 gas emissions for the historical period 1951–2005 and RCP-8.5 forcing scenario
153 for the future period (2006–2099) at 0.11° (≈ 12 km) horizontal resolution. This
154 simulation was a part of the coordinated activity by various institutions within
155 the Med-CORDEX phase-II framework. The Med-CORDEX focuses on coordi-
156 nated multi-model and multi-scenario studies covering the Mediterranean
157 region with high resolution coupled regional climate models (Ruti et al, 2016). As
158 the Mediterranean Sea plays an important role during the Vb-cyclone events,
159 first we compared the Mediterranean SST of our coupled simulations with ob-
160 servations (for the historical period) along with the Med-CORDEX ensemble
161 members.

162 We evaluate the EC-EARTH driven regional climate simulation with the
163 ECMWF twentieth century reanalysis (ERA-20C) driven coupled regional cli-
164 mate simulation for Vb-cyclone frequency and characteristics in the historical
165 period before we proceed to investigate the future Vb-cyclone characteris-
166 tics. Thereafter the North-Western Mediterranean Sea state in terms of SST,
167 evaporation & wind speed corresponding to the Vb-cyclone precipitation over
168 the three catchments, the Danube, Elbe and Odra in the two simulations

169 is analyzed. Finally to quantify the process chain linking the North-Western
170 Mediterranean Sea and the Vb-precipitation over the three catchments we use
171 information theory methods similar to the studies by Pothapakula et al (2019,
172 2020); Krug et al (2021b). These studies used information exchange to quan-
173 tify the Indo-Pacific coupling, the interplay between the Indian Ocean dipole &
174 El-Niño southern oscillations with the Indian Monsoon precipitation, and, the
175 role of North-Western Mediterranean Sea evaporation during the Vb-cyclone
176 precipitation over Odra catchment. More details about these methods and the
177 simulations are explained in the data and methodology section.

178 Specifically, we ask the following questions in this study:

179 1. Is the SST from the regional coupled simulation driven by the EC-
180 EARTH GCM comparable to the observed SST in the historical period. Fur-
181 thermore, does it produce future SST climate signals in line with the Med-
182 CORDEX phase-II ensemble?

183 2. Does the EC-EARTH driven coupled regional simulation produce Vb-
184 events comparable to the ERA-20C reanalysis driven coupled regional simula-
185 tion in the historical period. Do the Vb-cyclones change in the future?

186 3. Does the state of the North-Western Mediterranean Sea and the process
187 chain differ between the two simulations in the historical period & in the future
188 period?

189 This paper is organized as follows. Section 2 consists of data and method-
190 ology which describes the climate models, the Vb-cyclone tracking, and a brief
191 introduction to information theory methods. Thereafter, we present the results
192 and discussion in Section 3 which includes validation of the EC-EARTH driven
193 SST, the Vb-cyclones in historical and future periods. Results representing the
194 state of North-Western Mediterranean Sea & quantifying the process chain in-
195 terms of information exchange to the Vb-cyclone precipitation over the three
196 catchments are also presented in this section. Finally, some conclusions and
197 outlook are given in Section 4.

198 **2 Data and Methods**

199 **2.1 Regional Coupled Climate Model Setup**

200 The dynamical downscaling was performed with the regional climate model
201 COMSO-CLM 5-0-9 (Rockel and Geyer, 2008) as the atmospheric compo-
202 nent (Sevault et al, 2014). The COSMO-CLM is a non-hydrostatic regional
203 model designed for applications across various spatial and temporal scales.
204 The governing equations were numerically solved by the Runge Kutta time-
205 stepping scheme (Wicker and Skamarock, 2002). It used the Arakawa-C grid
206 in rotated geographical coordinates and follows terrain sigma vertical coordi-
207 nates. The horizontal resolution of COSMO-CLM was about 0.11° and used 40
208 vertical layers representing about 22.7 km of the atmospheric column. The ap-
209 plied physical parameterizations included the Ritter and Geleyn (1992) radiative
210 scheme, the Tiedtke convection scheme, and a four-category microphysics

211 scheme (Doms and Baldauf, 2011; Doms et al, 2011). The soil-vegetation-
212 atmosphere-transfer sub-model (TERRA-ML) provided the lower boundary
213 conditions over land. The current simulation used the AeroCom Global AOD
214 data (Kinne et al, 2006) to represent the aerosol properties. The initial and the
215 lateral boundary files were taken from the EC-EARTH available through the
216 SMHI Sweden (Hazeleger et al, 2012). The lateral boundary files were updated
217 every 6 hours for the entire simulation period (1951-2099).

218 The NEMOMED12 is the ocean component of the coupled regional climate
219 system (Sevault et al, 2014). The regional version of the NEMO-V2.6 was
220 adapted over the Mediterranean region named NEMOMED12. The domain of
221 the NEMOMED12 covers the entire Mediterranean Sea at a horizontal reso-
222 lution of $\approx 7.5\text{km}$ along with a buffer zone nearby the Atlantic Ocean. A 3D
223 relaxation of the temperature and salinity was performed at the buffer zone so
224 as to realistically simulate the circulation from the Atlantic through the strait
225 and into the Mediterranean Sea. The Black sea was parameterized such that
226 the resultant net balance of the water budget is added into the Mediterranean
227 Sea. The water budget was closed through the Total Runoff Integrating Path-
228 ways (TRIP) model (Oki and Sud, 1998) which supplies freshwater influx at
229 the Mediterranean river mouths. For more information on the NEMOMED12
230 readers are advised to refer Somot et al (2008); Sevault et al (2014). The
231 coupling of the sub-components in the regional coupled system was done by
232 OASIS-MCT3 coupler (Valcke, 2013).

233 We also discussed the results from a simulation with similar set-up (in addi-
234 tion to the Mediterranean Sea, North & Baltic Sea were additionally coupled)
235 but driven by the ECMWF twentieth century reanalysis, ERA-20C (Poli et al,
236 2016). The performance of ERA-20C downscaled simulation in realistically
237 replicating the Vb-cyclone events & their associated precipitation was already
238 reported and analyzed in the study by Krug et al (2021a). Hence in this study,
239 we used the ERA-20C downscaled simulation as a reference for validating the
240 downscaled EC-EARTH simulated Vb-cyclone events & their associated pre-
241 cipitation in the historical period. From hereafter the downscaled simulation
242 driven by ERA-20C is referred to as evaluation simulation, the downscaled
243 EC-EARTH simulation in the historical period (1951-2005) as historical sim-
244 ulation, and finally the future period (2045-2099) of downscaled EC-EARTH
245 simulation as a future simulation. Each of these simulations covered a period
246 of 55 years.

247 2.2 Observational data sets and Med-CORDEX ensemble members

248 To validate the SST obtained from the evaluation & historical regional cou-
249 pled simulations, we used the UK Met Office's Hadley Centre Sea Ice and Sea
250 Surface Temperature dataset (HadISST 1.1) (Rayner et al, 2003) in the histor-
251 ical period. In addition, we also used the NOAA Optimum Interpolation (OI)
252 SST V2 (Reynolds et al, 2002) as another source of observational data set.
253 Furthermore, as our downscaled simulation with EC-EARTH was a part of

254 coordinated activity contributing to the Med-CRODEX phase II simulations,
 255 we also used the SST data sets available from the Med-CORDEX phase-II
 256 database to evaluate our simulations. The institutions and the models are
 257 described in Table 1.

Table 1: RCMs/observations descriptions for SST evaluation over the Mediter-
 ranean Sea.

RCM Modeling Institution	Acronym	driving model
University of Belgrade	EBUPOM2c	MPI-ESM-LR
CNRM Meteo-France,Toulouse	CNRM-RCSM4	CNRM-CM5
Helmholtz-Zentrum Hereon, Geesthacht	GERICS-AWI-ROM44	MPI-ESM-LR
Helmholtz-Zentrum Hereon, Geesthacht	GERICS-AWI-ROM22	MPI-ESM-LR
Goethe-University Frankfurt (GUF)	CLMcom-GUF-CCLM5-0-9-NEMOMED12-3-6	EC-EARTH
Observations and Reanalysis data sets		
HadISST	–	–
OISST	–	–
Goethe-University Frankfurt (GUF)	CLMcom-GUF-CCLM5-0-9-NEMOMED12-3-6-NEMO-NORDIC-3.3	ERA-20C

258 The SST data sets from the models in Table 1 are available through the
 259 Med-CORDEX website (<https://www.medcordex.eu>). The University of Bel-
 260 grade used the Princeton Ocean Model (POM) as the regional ocean compo-
 261 nent and the limited area model Eta/NCEP for the atmospheric component
 262 (Djurdjevic and Rajkovic, 2008), the Centre National de Recherches Meteo-
 263 rologiques (CNRM), Meteo France used the NEMOMED8 as the ocean model
 264 and the ALADIN-Climate model as the atmospheric component (Sevault et al,
 265 2014). The GERICS-AWI Helmholtz-Zentrum Hereon Geesthacht, Climate
 266 Service Center Germany used the MPIOM developed at the Max Planck In-
 267 stitute for Meteorology (Hamburg, Germany) as the ocean component and
 268 REMO as the atmospheric component. All the SST data sets were interpo-
 269 lated onto a common grid prescribed by the Med-CORDEX community named
 270 OMED-11i which is approximately 12 km in resolution. Note that simulations
 271 obtained from the Med-CORDEX database were used only for evaluating the
 272 SST signal from our Goethe-University Frankfurt (GUF) simulations.

273 2.3 Vb-Cyclone tracking

274 For detecting & tracking Vb-cyclones we used a tracking algorithm developed
 275 by Wernli and Schwerz (2006) which was later modified by Sprenger et al
 276 (2017). We used the mean sea level pressure output from the dynamically
 277 downscaled ERA-20C, GUF evaluation simulation, the EC-EARTH driven
 278 GUF historical and future simulation as an input for the tracking algorithm (at
 279 a 6-hourly interval). Initially, within the domain, 25° W–45° E and 25° N–75°
 280 N, closed isobars were tracked and the deepest pressure within the closed
 281 isobar was considered to be the cyclone center. Thereafter, the next following
 282 track point cyclone center was selected by a guess on the past displacement

283 vector within a search of radius 1000 km. The tracking algorithm considers
284 all the cyclones crossing the 47° N latitude and between the longitudes, 12° E
285 and 22° E with a lifetime greater than 24 hours (Hofstätter et al, 2016; Wernli
286 and Schwierz, 2006). For more details regarding the tracking algorithm, the
287 readers are directed to refer Krug et al (2021a).

288 2.4 Vb-cyclones & North-Western Mediterranean Sea state

289 After the Vb-cyclone tracking in GUF simulations, we analyzed their frequency
290 of occurrence, track density, minimum central pressure, and precipitation. As
291 the Vb-cyclone are rare events, we considered 55 years in the historical and
292 future periods to account for sufficient Vb-cyclone cases. Hence the histori-
293 cal period was taken from 1951-2005 & the future period from 2045-2099 in
294 this study. The number of Vb-cyclone events per year along with their linear
295 trends and respective 95% confidence intervals was analyzed in the GUF eval-
296 uation, historical, and future simulations. The minimum central core pressures
297 obtained from the simulations were plotted using box whiskers.

298 For the Vb-precipitation analysis, we selected three important catchments
299 i.e., the Danube, Elbe, and Odra (shown as rectangles in black, orange, and
300 green colors respectively in Figure 3). The area-averaged precipitation sum
301 anomaly accumulated during the Vb-cyclone days over these catchments was
302 further ranked according to the intensity. The precipitation sum anomaly dur-
303 ing the Vb-event was calculated by subtracting the day sum with the clima-
304 tology day sum precipitation in the GUF evaluation, historical, and future
305 simulations respectively. In addition to the Vb-cyclone precipitation anomaly
306 rankings, we also showed the absolute precipitation amounts.

307 Corresponding to the Vb-cyclone precipitation anomaly rankings we an-
308 alyzed the state of the North-Western Mediterranean Sea (7° E, 22° E, 35°
309 N, 46° N) similar to the study by Krug et al (2021a). The corresponding spa-
310 tially and temporally averaged SST, evaporation, and wind speeds anomalies
311 over this region were plotted corresponding to the Vb-cyclone precipitation
312 anomaly rankings in GUF evaluation, historical, and future simulations. We
313 also showed the moving averages of SST, evaporation, and wind speed anoma-
314 lies for 10 Vb-events with the Local Polynomial Regression Fitting (LOESS)
315 lines corresponding to the precipitation anomalies over the Danube, Elbe, and
316 Odra catchments. We adapted the methodology as in Krug et al (2021a) for an-
317 alyzing the precipitation rankings and corresponding North-Western Mediter-
318 reanean Sea state.

319 2.5 Quantifying process chain between North-Western Mediterranean Sea & 320 Vb-cyclone precipitation

321 Methods from information theory were recently used in quantifying interac-
322 tions among sub-systems, especially in climate (Pothapakula et al, 2019, 2020;

323 Krug et al, 2021b; Ruddell et al, 2019). Transfer entropy (TE) was especially
 324 used in detecting and quantifying the direction of information exchange be-
 325 tween two or more sub-systems. Unlike correlation, TE is an asymmetrical
 326 measure. Furthermore, the estimations from TE are free from any underly-
 327 ing assumptions of the probability distributions. Though the TE is a useful
 328 measure, its estimation is still a challenge.

329 A study by Pothapakula et al (2019) tested various TE estimators on ide-
 330 alized and real climate test cases along with the sensitivity of these estimators
 331 on time series length. Their results showed that the TE-linear which assumes
 332 Gaussianity is robust in revealing the system dynamics. While the non-linear
 333 estimations like TE Kraskov, Kernel gave reliable results, free-tuning param-
 334 eters such as the number of nearest neighbors, kernel width were tested and
 335 tuned for reliable estimations.

336 In this study, we used the robust TE-linear estimation to quantify the
 337 process chain in terms of information exchange between the North-Western
 338 Mediterranean Sea and the spatio-temporal averaged precipitation over three
 339 catchments during the detected Vb-events. Krug et al (2021b) applied the
 340 same methodology to quantify the information exchange between the North-
 341 Western Mediterranean Sea and the precipitation over Odra catchments during
 342 Vb-cyclones.

343 At the heart of the information theory lies the concept of Entropy (H). The
 344 Entropy quantifies the uncertainty of a random variable X (Shannon, 1948)
 345 and is defined as,

$$H(X) = - \sum_x p(x) \log p(x), \quad (1)$$

346 where $p(x)$ represents the probability of a state of the random variable X .
 347 The summation goes through all the states of the random variable quantifying
 348 the average uncertainty of X . The units of entropy are generally expressed
 349 in nats when natural logarithm is used, whereas in the units of bits if the
 350 logarithm to the base of 10 is used. In this study, all the results quantifying
 351 information exchange were expressed in the units of nats.

352 Mutual information (MI) is defined as the average uncertainty reduction
 353 in the random variable X provided by the knowledge of random variable Y or
 354 vice-versa.

$$MI_{XY} = \sum_{x,y} p(x,y) \log \frac{p(x,y)}{p(x)p(y)}, \quad (2)$$

355 Where the $p(x,y)$ represents the joint probability of a state corresponding
 356 to the random variables X and Y . The MI is a symmetric quantity and thus
 357 can not detect the direction of information exchange.

358 The TE builds upon the MI measure and is defined as mutual informa-
 359 tion between the future target variable X and the whole past of the source
 360 Y^- conditioned on the whole past of the target variable X^- . The TE is an
 361 asymmetric measure giving directional information exchange.

$$TE_{Y \rightarrow X} = MI(X; Y^- | X^-). \quad (3)$$

Due to computational complexity in the estimation of joint probability densities, the whole past of the source and target random variables are reduced as follows,

$$TE_{Y \rightarrow X} = MI(X; Y_{t-\tau} | X_{t-\omega}), \quad (4)$$

where τ and ω represents the time lags of the history of source and target variables. The values of the τ and ω are generally chosen depending on the system dynamics. For more detailed review on TE and its estimation refer to Pothapakula et al (2019).

In this study, we chose the target variable to be the spatial averaged daily precipitation anomaly over the respective catchments during a Vb-cyclone event and the source being the simultaneous state of SST, evaporation or wind speed anomalies over the North-Western Mediterranean Sea. The value of τ was taken to be zero and ω as one consistent to the study of Krug et al (2021b). The TE measure in this study quantifies the reduction in uncertainty about the present state of precipitation in the respective catchment while knowing the state of North-Western Mediterranean Sea (SST, evaporation or wind speed) during the same day given the knowledge of one day precipitation persistence in the catchment region. Significance tests with permuted surrogates were conducted for information exchange values (Lizier, 2014; Pothapakula et al, 2019). As the measure of TE is highly sensitive to the time series length, the Vb-cyclone events detected within 55 year period were used instead of a typical 30 year period.

3 Results and discussion

In this section, first, the SST's obtained from the GUF historical simulation, GUF evaluation simulation, and additionally the Med-CORDEX phase-II ensemble members are compared against observations. Thereafter, we discuss the simulated climate change signal of the Mediterranean SST. Thereafter, the Vb-cyclone detection in the GUF historical & evaluation simulations along with GUF future simulation will be discussed. Finally we analyze the North-Western Mediterranean Sea state and associated process chain interms of information exchange during these events.

3.1 Evaluation & future projections of Mediterranean SST

Figure 1a shows the temporal evolution of the basin averaged annual Mediterranean SST for various simulations. Comparing the GUF historical & GUF evaluation simulated SST's to the HadISST & OISST observational data sets, we noticed a cold bias ($\approx 1 - 1.5$ K). This cold bias was more pronounced

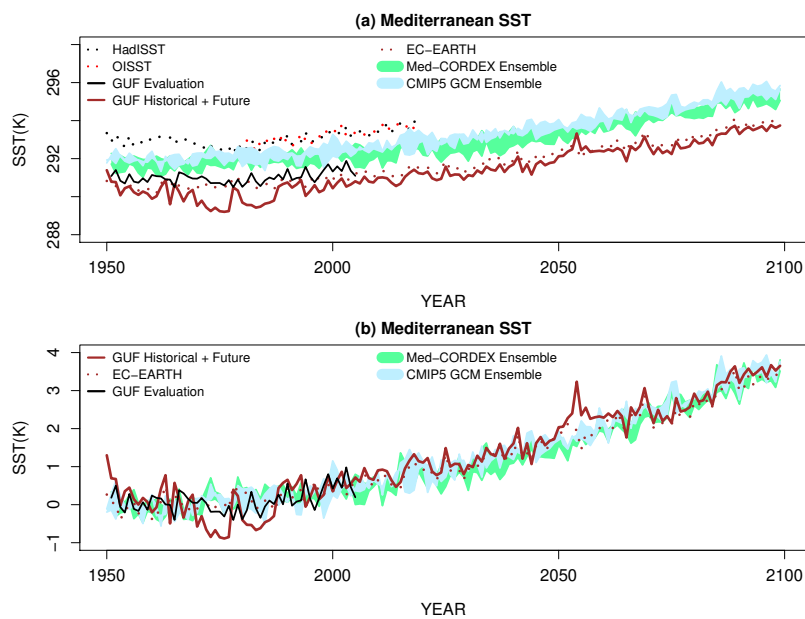


Fig. 1: (a) Mediterranean Sea basin averaged annual SST (K) evolution and (b) SST anomalies for the time period 1951-2099 (with reference to historical period 1951-2005) obtained from various simulations along with observational data sets, the HadISST & OISST.

397 in the GUF historical compared to the GUF evaluation simulation. This may
 398 be attributed to a more realistic atmospheric forcing by COSMO-CLM on the
 399 ocean model NEMOMED12 in the evaluation simulation compared to historical
 400 simulation. The Med-CORDEX phase-II ensemble also simulated a cold
 401 bias, but a smaller one compared with GUF simulations. A closer look into the
 402 seasonal cycle revealed that almost all the simulations had a cold bias in the
 403 spring & summer seasons (Fig. S1 in supplementary material). It was interest-
 404 ing to note the close correspondence of the driving GCM's and the downscaled
 405 simulated SST time evolution in Fig. 1a. The global model, EC-EARTH's SST
 406 was colder than the other considered CMIP5 GCM SST's, hence, this explains
 407 the comparably larger cold bias of the GUF historical simulation. Furthermore,
 408 a narrow spread in the Med-CORDEX ensemble and CMIP5 GCM ensemble
 409 was identified. Selection of only two GCM's for downscaling, i.e., the MPI-
 410 ESM-LR and CNRM from the CMIP5 simulations so far might the reason for
 411 such a narrow spread.

412 A closer look into the spatial SST and the bias plots in historical period
 413 revealed that the cold bias was present throughout the Mediterranean Sea
 414 (Fig. S2 & Fig. S3 in supplement). Especially the south-eastern warm pool

415 was not very well captured by the GUF simulations and also by the Med-
416 CORDEX ensemble members. However, overall important SST patterns (e.g.,
417 the warm eastern pool in the Levantine compared to the western cold pool
418 over the North-Western Mediterranean) of the Mediterranean Sea were well
419 captured by the GUF evaluation & GUF historical simulations.

420 The Mediterranean SST climate change signal is presented in Fig. 1b. The
421 SST anomaly was calculated with respect to the reference period 1951-2005.
422 Almost all the simulations agreed very well that the basin averaged Mediter-
423 ranean SST will warm ≈ 2.5 K – 3 K under the RCP-8.5 scenario by the end
424 of 21st century. This warming of the Mediterranean Sea is consistent with the
425 findings by Soto-Navarro et al (2020). Spatial climate change SST patterns
426 in GUF and the Med-CORDEX ensemble simulations reveal a homogeneous
427 warming throughout the Mediterranean Sea (Fig. S4 in supplement). As the
428 GUF simulations captured the SST signals and spatial patterns in-line with the
429 observations & Med-CORDEX ensemble in the historical & future periods, we
430 proceed further to explore the Vb-cyclones, the North-Western Mediterranean
431 Sea state and associated process chains in the subsequent sections.

432 3.2 Vb-cyclones in the historical and future periods

433 In this sub-section, we present and discuss the results obtained from Vb-
434 cyclone tracking in various GUF simulations. For the GUF evaluation simula-
435 tion, a total of 531 Vb-cyclone events were detected for the period 1951-2005
436 corresponding to 9.7 (standard deviation ≈ 2.1 events per year) Vb-cyclone
437 events per year. In the GUF historical simulation, a total of 557 Vb-cyclone
438 events were detected for the period 1951-2005 corresponding to 10.1 Vb-events
439 per year (standard deviation ≈ 1.6 events per year). The GUF historical sim-
440 ulation slightly overestimated the number of Vb-events by a statistically in-
441 significant amount of 4.8% compared to the GUF evaluation. With respect
442 to the seasonal differences, on average the GUF historical simulation overesti-
443 mated the Vb-cyclone occurrence by 49% per year in summer (significant at
444 95% confidence) while in winter it underestimated Vb-cyclones by 41% per
445 year (significant at 95% confidence) compared to GUF evaluation. No signifi-
446 cant trends were revealed in GUF historical & evaluation simulations for the
447 whole period (Fig .2).

448 In total 567 Vb-cyclones were detected in the GUF future simulation for
449 the period 2045-2099 corresponding to 10.3 Vb-cyclones per year (standard
450 deviation ≈ 2.3 events per year). This indicates an increase by 1.8% Vb-
451 cyclones events per year in the future period compared to the historical period.
452 Standard student's t-test analysis revealed that this percentage increase was
453 insignificant. This result is consistent with the findings by Mittermeier et al
454 (2019) where an insignificant percentage increase of Vb-cyclone frequency in
455 the far future was reported with 0.11° resolution stand-alone regional climate
456 model. No significant changes in the Vb-cyclone seasonal frequency & trends

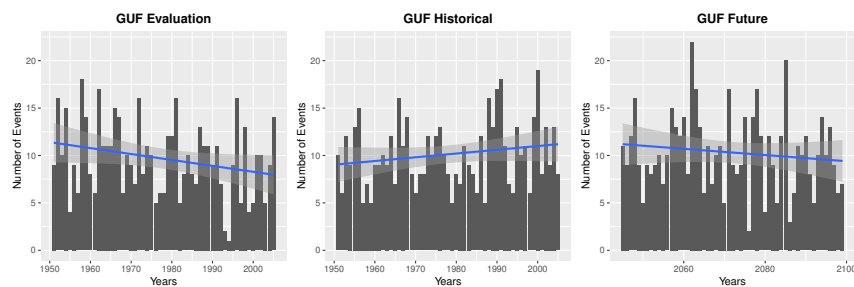


Fig. 2: Time series of annual Vb-cyclone event number and their associated trends for the GUF evaluation, historical, and future simulations. The shaded intervals correspond to the 95% confidence intervals for the Vb-event trend line.

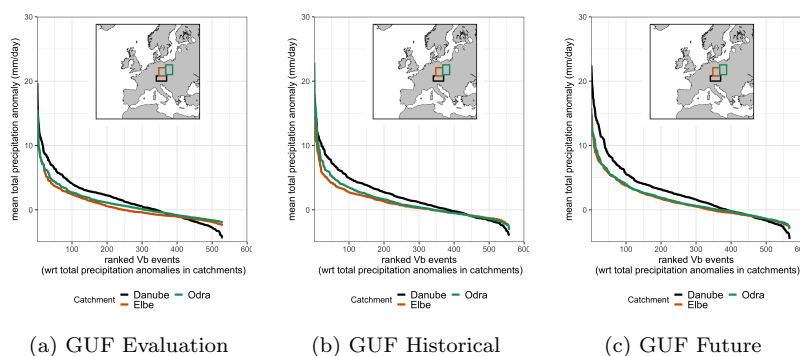


Fig. 3: Ranked Vb-cyclone total precipitation anomalies in the Danube, Elbe, and Odra catchments obtained from various GUF simulations.

457 were revealed in the future simulation compared to historical simulation (Fig.
458 S5 in supplement).

459 A good agreement in the Vb-cyclone track density was also detected be-
460 tween the GUF historical & GUF evaluation (Fig. S6 in supplement). However,
461 a minor underestimation of $\approx 1\%$ of the Vb-cyclone centers over the eastern
462 flanks of the Alps and a very slight overestimation over Italy was noted in
463 the GUF historical simulation. In the simulated future, the Vb-cyclones trav-
464 elled further north-eastwards compared to the historical period (also reported
465 in Messmer et al (2020)). The Vb-cyclones intensity in terms of mean mini-
466 mum cyclone central pressure also revealed good agreement between the GUF
467 historical & GUF evaluation simulation (Fig. S7 & Fig. S8 in supplement).
468 The GUF future simulation indicated no significant changes in the Vb-cyclone
469 mean minimum central pressures in the future compared to historical simu-
470 lation.

471 Figure 3 shows the Vb-cyclone precipitation anomalies ranked according
472 to their magnitudes (lowest rank for maximum anomaly) in the Danube, Elbe,

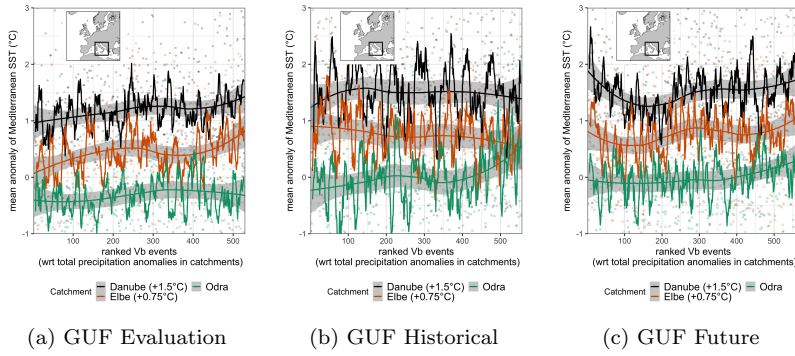


Fig. 4: Sea surface temperature anomalies corresponding to the Vb-cyclone precipitation anomaly rankings in various GUF simulations for Danube, Elbe and Odra catchments. The lines show the moving average and the LOESS regression. The data for Danube and Elbe catchments were shifted by constant values for improved representation.

473 and Odra river catchments for various GUF simulations. The rankings over
 474 the Elbe & Odra catchments in GUF evaluation showed similar anomaly mag-
 475 nitudes due to their close spatial proximity. The Danube catchment showed
 476 higher precipitation anomalies in high & medium ranks ($\approx > 400$ ranks) while
 477 a higher variability in lower ranks compared to Elbe & Odra. This behavior
 478 of Danube was attributed to the presence of complex orography and also to
 479 the typical Vb-cyclone pathways (Krug et al (2021a)). There is a good agree-
 480 ment between the GUF evaluation & GUF historical simulated precipitation
 481 rankings over all three catchments. Furthermore, a good agreement in abso-
 482 lute precipitation amounts and in the spatial precipitation patterns were found
 483 between the GUF historical & GUF evaluation (Fig. S9 & Fig. S10 in suppl-
 484 ement). However the precipitation magnitudes for a few high-ranked events (\approx
 485 1-20 ranks) were greater ($\approx 0.5, 0.45, 0.25$ mm/day) in the Danube, Elbe, and
 486 Odra catchments respectively in GUF evaluation simulation. No significant
 487 differences were found in the future precipitation anomalies and magnitudes
 488 (Fig. S10 & Fig. S11 in supplement).

489 3.3 North-Western Mediterranean Sea state during the Vb-cyclones & 490 associated process chains

491 This sub-section presents the state of the SST, evaporation, and wind speed
 492 anomalies over the North-Western Mediterranean Sea & associated process
 493 chains interms of information exchange.

494 Figure 4 shows the spatially averaged SST anomalies of the North-Western
 495 Mediterranean Sea (domain shown in black rectangle box) with respect to the
 496 Vb-cyclone precipitation anomaly rankings. In the GUF evaluation simulation
 497 the high precipitation anomalies tend to be realized for low SST anomalies,

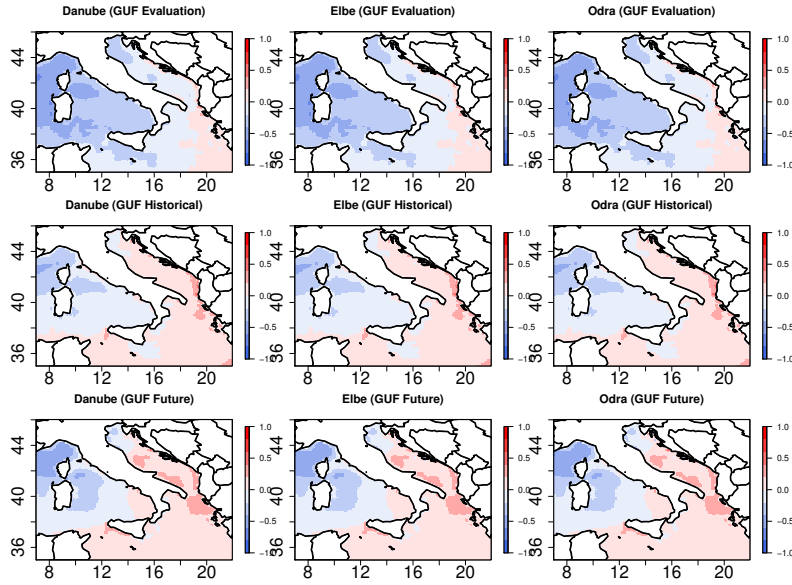


Fig. 5: Mean sea surface temperatures anomalies (K) during all the Vb-cyclones in various GUF simulations corresponding to precipitation over Danube, Elbe and Odra catchments.

498 especially for the Danube and Elbe catchments. This might be attributed to
 499 the strong upper sea mixing and evaporative cooling. These cooler anomalies
 500 were also partially replicated for the Danube & Odra basins in the GUF his-
 501 torical (≈ 1 -100 ranks). In the GUF future simulation the SST cooling was not
 502 noticed. Figure 5 presents the spatial distribution of the mean SST anom-
 503 alies over the North-Western Mediterranean Sea during all the Vb-events. The
 504 GUF evaluation simulation on average showed negative SST anomalies in the
 505 North-Western Mediterranean Sea. This was expected as the Vb-cyclones usu-
 506 ally originate from the North-Western Mediterranean Sea. Though the cool-
 507 ing in the GUF historical simulation was noticed with less magnitude in the
 508 North-Western domain, no such cooling was seen over the Adriatic sea & Ion-
 509 ian region. This means that the SST's in these regions were not responsive in
 510 the GUF historical simulation. This behaviour was also seen in the bias plots,
 511 where the cooling of the SST's in the GUF historical was underestimated com-
 512 pared to GUF evaluation (Fig. S12 in supplement). The difference between the
 513 future and historical simulations on average showed no major differences in the
 514 magnitude of SST cooling during Vb-cyclones.

515 Thereafter, we investigated the information exchange between the SST's
 516 and the Vb-cyclone precipitation over the three catchments to diagnose the
 517 process chains (Fig. 6). We noted differences in the information exchange spa-
 518 tial locations between the GUF evaluation & historical simulations, especially

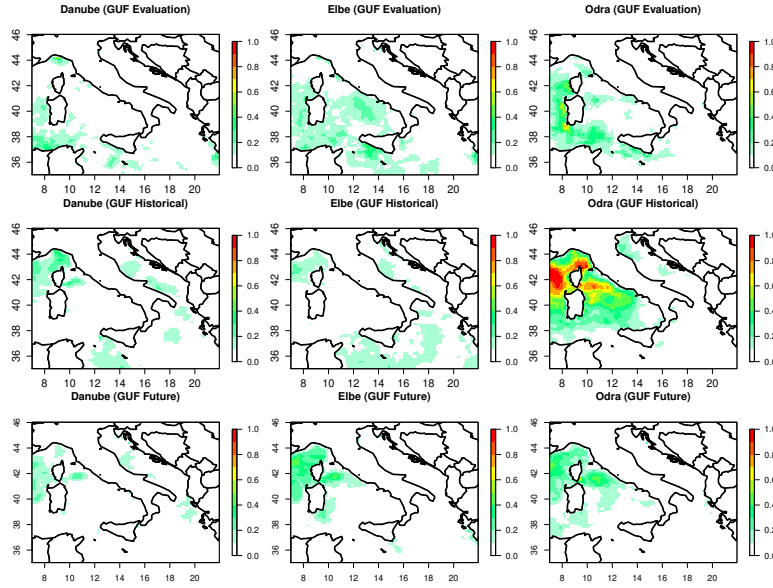


Fig. 6: Information exchange ($\times 10^{-2}$ nats) between the SST's and the total precipitation anomalies over the Danube, Elbe and Odra catchments for various GUF simulations. Only 95% significant range is plotted.

519 in the Elbe and Odra catchments. In the GUF historical simulation an underestimation of information exchange between the North-Western Mediterranean
 520 and the precipitation over the Elbe, and an overestimation in the information
 521 exchange over the Odra catchments was seen. The spatial locations of the in-
 522 formation exchange in the future simulation remained the same as in historical
 523 simulation, but with minor changes in the magnitude of information exchange.
 524

525 Figure 7 shows the evaporation anomalies over the North-Western Mediter-
 526 ranean Sea. In the GUF evaluation simulation the evaporation anomalies cor-
 527 responded to the precipitation anomaly rankings in all the catchments indicat-
 528 ing the dependence of Vb-cyclones on the North-Western Mediterranean Sea
 529 moisture. The GUF historical simulation shows no such correspondence except
 530 for only a minor increase in the anomalies of evaporation over the Danube and
 531 Elbe catchment (high ranks, $\approx > 100$ ranks). The spatial plots in Fig. 8 show
 532 that on average the evaporation over the North-Western Mediterranean sea
 533 was underestimated in the GUF historical simulation during the Vb-events,
 534 specially, over the Adriatic & Ionian regions. This was further evident from
 535 the bias plots (Fig. S13 in supplement). The spatial patterns corresponding to
 536 the GUF future simulations on average showed no changes in the magnitude
 537 of evaporation anomalies compared to the historical period.

538 The information exchange between the evaporation over the North-Western
 539 Mediterranean Sea and the Vb-cyclone precipitation over the three catch-

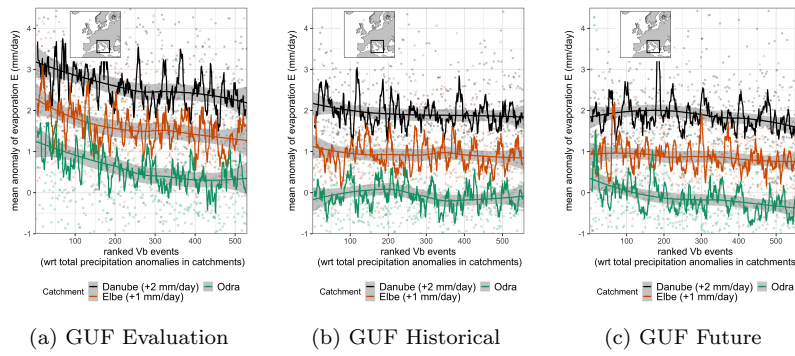


Fig. 7: Evaporation anomalies corresponding to the Vb-cyclone precipitation anomaly ranking in various GUF simulations for Danube, Odra and Elbe catchments. The lines show the moving average and the LOESS regression. The data for Danube and Elbe catchments were shifted by constant values for improved representation.

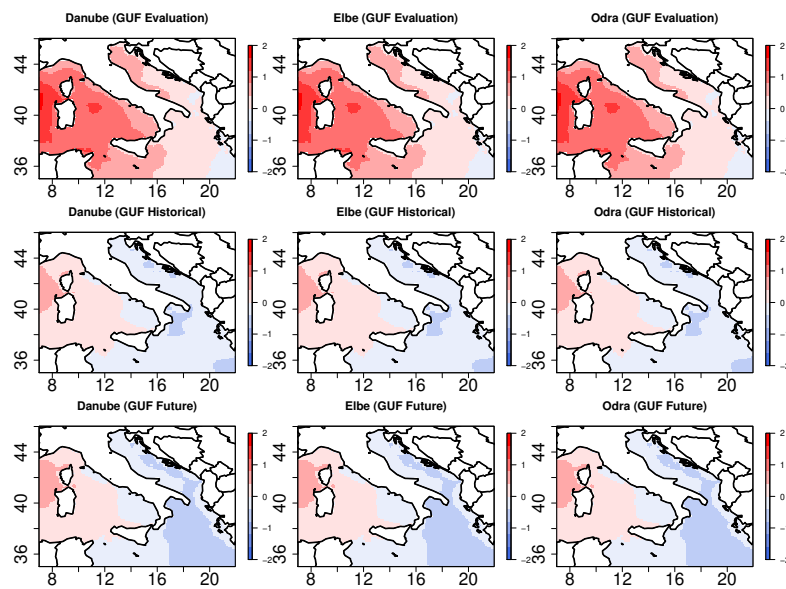


Fig. 8: Mean anomaly patterns of evaporation (mm/day) over the Mediterranean Sea from various GUF simulations for all Vb-cyclone events.

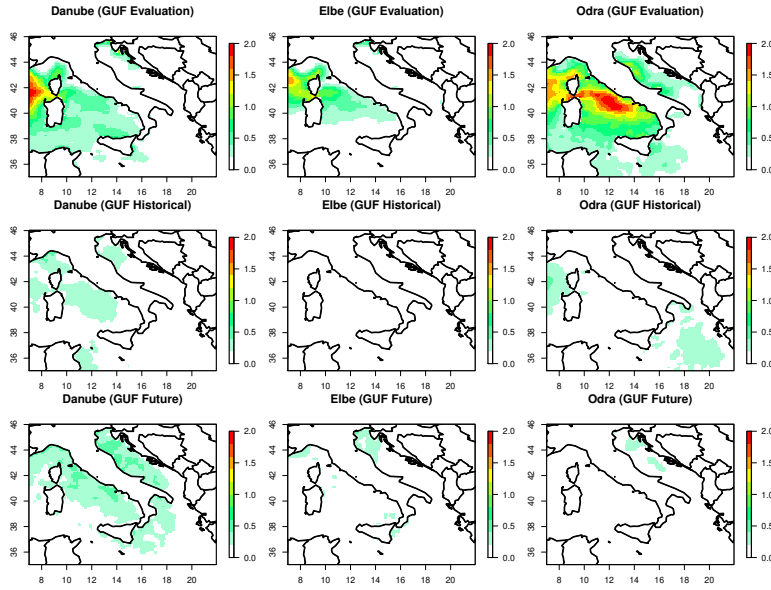


Fig. 9: Information exchange ($\times 10^{-2}$ nats) between the evaporation over the Mediterranean Sea and the total precipitation anomalies over the Danube, Elbe and Odra catchments for various GUF simulations. Only 95% significant range is plotted.

540 ment's is presented in Fig. 9. We noticed significant information exchange
 541 between the North-West Mediterranean basin evaporation (and also Adriatic
 542 Sea for Odra catchment) and the Vb-cyclone precipitation in GUF evaluation
 543 simulation for all the catchments. This behavior was not replicated in the GUF
 544 historical simulation. This indicates that some crucial physical process linking
 545 the evaporation and Vb-cyclone precipitation were missing in GUF historical
 546 simulation. The information exchange spatial locations do vary between the
 547 GUF historical & GUF future but the difference in magnitudes of information
 548 exchange is less compared to the differences between the GUF historical &
 549 GUF evaluation simulations.

550 Figure 10 shows the wind-speed anomalies corresponding to the Vb-cyclone
 551 precipitation anomaly rankings. The high wind speed anomalies tend to be
 552 realized for high precipitation rankings in GUF evaluation simulation. Krug
 553 et al (2021a) showed that these strong winds enhance the evaporation over the
 554 Mediterranean Sea fueling the Vb-cyclones especially during their initial phase.
 555 The increasing trends in wind-speed were also replicated in the GUF historical
 556 & GUF future simulations. However, the wind speed anomaly magnitudes were
 557 lower in GUF historical & future compared to the GUF evaluation simulation.

558 The spatial plots of the mean daily wind speed anomalies are shown in
 559 Fig. 11. On average the wind speed anomaly magnitudes in the GUF eval-

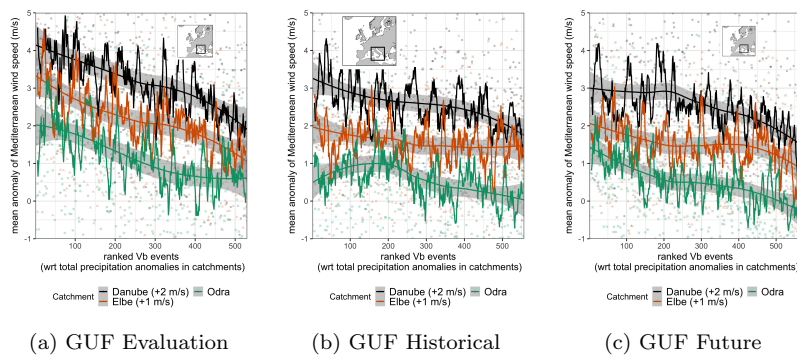


Fig. 10: Wind speed anomalies corresponding to the precipitation anomaly rankings in various GUF simulations for all Vb-events. The lines show the moving average and the LOESS regression. The data for Danube and Elbe catchments were shifted by constant values for improved representation.

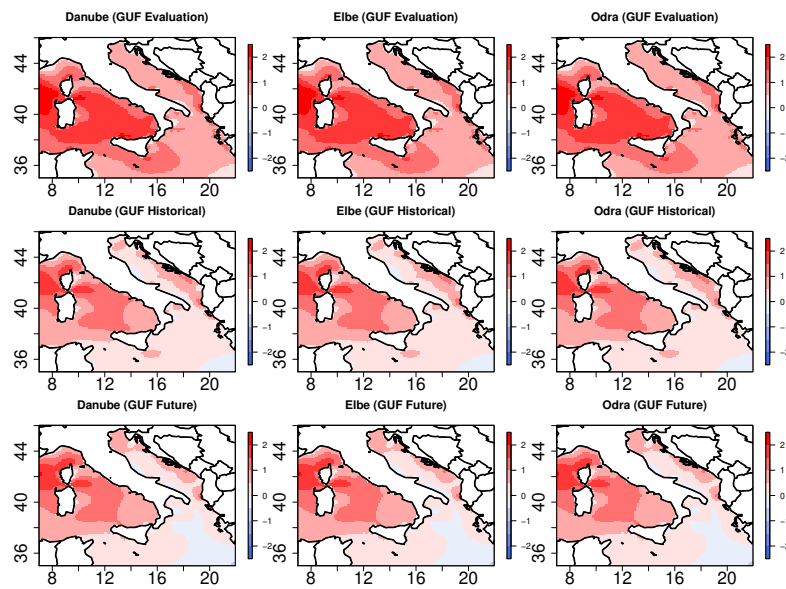


Fig. 11: Mean anomalies of wind speed (m/s) over the Mediterranean Sea in the GUF evaluation, historical, and future simulations over Danube, Elbe and Odra catchments for all Vb-cyclone events.

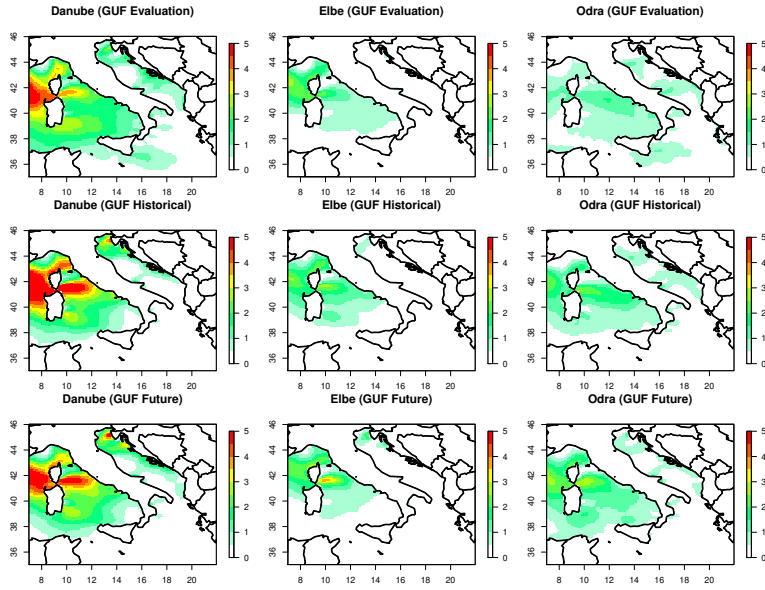


Fig. 12: Information exchange ($\times 10^{-2}$ nats) between the wind speed and total precipitation anomalies for various GUF simulations. Only 95% significant range is plotted.

560 uation simulation over the North-Western Mediterranean Sea were higher in
 561 magnitude compared to the GUF historical simulation. Also the spatial extent
 562 of the high magnitude winds during the Vb-cyclones extended from the
 563 North-Western Mediterranean Sea down to Ionian basin and the Adriatic Sea.
 564 This behavior was not replicated in the GUF historical simulation. This was
 565 further evident and conclusive from the bias plot (Fig. S14 in supplement).
 566 This evidence further indicates that during the Vb-cyclones in GUF historical
 567 simulation, the Adriatic and some parts of the Ionian basin were missing
 568 crucial feed-backs from the North-Western Mediterranean Sea. On average
 569 the difference in the magnitudes between the GUF future & GUF historical
 570 were very less compared with the difference between the GUF historical &
 571 GUF evaluation. The information exchange spatial locations and magnitude
 572 between the wind speed and the Vb-cyclone precipitation anomalies matched
 573 well in the GUF evaluation & GUF historical simulations compared with the
 574 SST and evaporation patterns (Fig. 12). A minor difference was noted between
 575 the GUF future and GUF historical simulations.

4 Conclusions

The current work focused on the Vb-cyclones and the corresponding North-Western Mediterranean Sea state & process chains as simulated in two coupled regional climate model simulations. One regional simulation was driven by ERA-20C reanalysis (1951-2005) called GUF evaluation, and the other simulation was driven by EC-EARTH for the period 1951-2099. The simulation for the period 1951-2005 was referred as GUF historical, and from the period 2006-2099 as GUF future.

The results revealed that GUF historical, GUF evaluation & the Med-CORDEX ensemble members considered in our study were cold ($\approx 1 - 1.5$ K) compared to the HadISST and OISST observation based datasets during the period 1951-2005. However, the major Mediterranean Sea SST patterns were well captured by the GUF simulations. All the regional climate simulated basin averaged SSTs closely followed the GCM simulated SST values reiterating the importance of the choice of the driving GCM which is dynamically downscaled. All the Med-CORDEX ensemble members agreed on the Mediterranean basin averaged SST warming of $\approx 2.5 - 3$ K by the end of the 21st century under the RCP-8.5 scenario compared to the historical period.

A good agreement was found in the Vb-cyclone frequency between the GUF evaluation (9.7 events per year) & GUF historical simulations (10.1 events per year). Also, the Vb-cyclone track density and intensity in terms of minimum cyclone central pressure showed good agreement. Moreover, the Vb-cyclone precipitation anomaly magnitude rankings also showed good agreement between the GUF evaluation & historical simulations. An insignificant increase by 1.8 % in the Vb-cyclone frequency by the end of 21st century was revealed from GUF future simulation. Changes in the future Vb precipitation anomalies over the three catchments were also insignificant.

In the GUF evaluation simulation the North-Western Mediterranean SST, evaporation, and windspeed anomalies corresponded to the Vb-cyclone precipitation anomaly rankings. Such a correspondence was not detected in the EC-EARTH driven historical simulation. Despite similarities in the model set-up (same regional atmosphere/ocean model components and set-ups over Mediterranean Sea) & good agreement in the Vb-cyclone frequency, intensity, and precipitation between the GUF evaluation & GUF historical simulation, the North-Western Mediterranean Sea state and process chains differ. These differences might be attributed to the emergence of simulation biases inherited from the driving EC-EARTH GCM, e.g., cold surface & sea surface temperatures over the Mediterranean compared to ERA-20C forcing. A study by Pothapakula et al (2020) showed that the biases in the driving GCMs emerged into the regional climate simulations resulting in unrealistic process chains. Downscaling the EC-EARTH3 (latest version of EC-EARTH) which has smaller bias in the surface air temperatures, SST (Döscher et al, 2021) might assist in further understanding the state and process chains linking the North-West Mediterranean Sea and the Vb-cyclone precipitation in historical & future periods.

621 **Acknowledgements** The financial support of the German Research Foundation (Deutsche
622 Forschungsgemeinschaft, DFG) in terms of the research group FOR 2416 Space-Time Dy-
623 namics of Extreme Floods (SPATE) is gratefully acknowledged. B.A and A.O would like to
624 thank the European Union’s Horizon 2020 research and innovation program, SOCLIMPACT
625 (DownScaling CLimate imPACTs and decarbonisation pathways in EU islands and en-
626 hancing socioeconomic and non-market evaluation of Climate Change for Europe, for 2050
627 and beyond) for the support. The authors acknowledge the Deutsches Klimarechenzentrum
628 (DKRZ) and the Hessian Competence Center for High Performance Computing. The simu-
629 lations were conducted as a part of Med-CORDEX initiative. The authors would also like
630 to thank all the institutions which provided SST data through the Med-CORDEX website.

631 **Declarations**

- 632 – **Availability of data and materials:** The SST data can be obtained from
633 the Med-CORDEX data base, <https://www.medcordex.eu> . The analysis
634 is done in R and all the codes used in this paper can be accessed through
635 10.5281/zenodo.5753360. The cyclone tracking method is available on re-
636 quest from Michael Sprenger.
- 637 – **Conflict of interest:** All the authors declare no conflict of interest.
- 638 – **Authors contribution** The concept was proposed by BA. Funding was
639 acquired by BA. The information theory algorithms were developed by
640 PKP. The RCM simulations were performed by AOH and PKP with the
641 assistance from TK. The paper was written by PKP and reviewed by all
642 the authors. All authors have read and approved the final paper.

643 **References**

- 644 Akhtar N, Brauch J, Ahrens B (2018) Climate modeling over the mediter-
645 ranean sea: impact of resolution and ocean coupling. *Climate Dynamics*
646 51(3):933–948
- 647 Akhtar N, Krug A, Brauch J, Arsouze T, Dieterich C, Ahrens B (2019) Eu-
648 ropean marginal seas in a regional atmosphere–ocean coupled model and
649 their impact on vb-cyclones and associated precipitation. *Climate Dynam-*
650 *ics* 53(9):5967–5984
- 651 Asharaf S, Ahrens B (2015) Indian summer monsoon rainfall processes in
652 climate change scenarios. *Journal of Climate* 28(13):5414–5429
- 653 van Bebber W (1891) Die Zugstrassen der barometrischen Minima nach den
654 Bahnenkarten der deutschen Seewarte für den Zeitraum 1875-1890
- 655 Beniston M, Stephenson DB, Christensen OB, Ferro CA, Frei C, Goyette S,
656 Halsnaes K, Holt T, Jylhä K, Koffi B, et al (2007) Future extreme events
657 in european climate: an exploration of regional climate model projections.
658 *Climatic change* 81(1):71–95
- 659 Blöschl G, Nester T, Komma J, Parajka J, Perdigão RA (2013) The june 2013
660 flood in the upper danube basin, and comparisons with the 2002, 1954 and
661 1899 floods. *Hydrology and Earth System Sciences* 17(12):5197–5212

- 662 Brogli R, Kröner N, Sørland SL, Lüthi D, Schär C (2019) The role of hadley
663 circulation and lapse-rate changes for the future european summer climate.
664 *Journal of Climate* 32(2):385–404
- 665 Cornes RC, van der Schrier G, van den Besselaar EJ, Jones PD (2018) An en-
666 semble version of the e-obs temperature and precipitation data sets. *Journal*
667 *of Geophysical Research: Atmospheres* 123(17):9391–9409
- 668 Djurdjevic V, Rajkovic B (2008) Verification of a coupled atmosphere-ocean
669 model using satellite observations over the adriatic sea. In: *Annales Geo-*
670 *physicae, Copernicus GmbH, vol 26, pp 1935–1954*
- 671 Doms G, Baldauf M (2011) A description of the nonhydrostatic regional cosmo-
672 model–part i: Dynamics and numerics consortium for small-scale modelling.
673 *Deutscher Wetterdienst, Offenbach, Germany*
- 674 Doms G, Förstner J, Heise E, Herzog H, Mironov D, Raschendorfer M, Rein-
675 hardt T, Ritter B, Schrodin R, Schulz JP, et al (2011) A description of the
676 nonhydrostatic regional cosmo model, part ii: Physical parameterization.
677 *Deutscher Wetterdienst, Offenbach, Germany*
- 678 Döscher R, Acosta M, Alessandri A, Anthoni P, Arneth A, Arsouze T,
679 Bergmann T, Bernadello R, Bousetta S, Caron LP, et al (2021) The ec-
680 earth3 earth system model for the climate model intercomparison project 6.
681 *Geoscientific Model Development Discussions* pp 1–90
- 682 Drobinski P, Da Silva N, Bastin S, Mailler S, Muller C, Ahrens B, Christensen
683 OB, Lionello P (2020) How warmer and drier will the mediterranean region
684 be at the end of the twenty-first century? *Regional Environmental Change*
685 20(3):1–12
- 686 Evans JP, Di Virgilio G, Hirsch AL, Hoffmann P, Remedio AR, Ji F, Rockel B,
687 Coppola E (2021) The cordex-australasia ensemble: evaluation and future
688 projections. *Climate Dynamics* 57(5):1385–1401
- 689 Fischer EM, Beyerle U, Knutti R (2013) Robust spatially aggregated projec-
690 tions of climate extremes. *Nature Climate Change* 3(12):1033–1038
- 691 Gangoiti G, Sáez de Cámara E, Alonso L, Navazo M, Gómez M, Iza J, García
692 J, Ilardia J, Millán M (2011) Origin of the water vapor responsible for the
693 european extreme rainfalls of august 2002: 1. high-resolution simulations
694 and tracking of air masses. *Journal of Geophysical Research: Atmospheres*
695 116(D21)
- 696 Giorgi F (2006) Climate change hot-spots. *Geophysical research letters* 33(8)
- 697 Harris I, Osborn TJ, Jones P, Lister D (2020) Version 4 of the cru ts monthly
698 high-resolution gridded multivariate climate dataset. *Scientific data* 7(1):1–
699 18
- 700 Hazeleger W, Wang X, Severijns C, Ştefănescu S, Bintanja R, Sterl A, Wyser
701 K, Semmler T, Yang S, Van den Hurk B, et al (2012) Ec-earth v2. 2: de-
702 scription and validation of a new seamless earth system prediction model.
703 *Climate dynamics* 39(11):2611–2629
- 704 Hentgen L, Ban N, Kröner N, Leutwyler D, Schär C (2019) Clouds in
705 convection-resolving climate simulations over europe. *Journal of Geophys-*
706 *ical Research: Atmospheres* 124(7):3849–3870

- 707 Hofstätter M, Chimani B (2012) Van bebbber’s cyclone tracks at 700 hpa in
708 the eastern alps for 1961-2002 and their comparison to circulation type
709 classifications. *Meteorologische Zeitschrift* pp 459–473
- 710 Hofstätter M, Chimani B, Lexer A, Blöschl G (2016) A new classification
711 scheme of european cyclone tracks with relevance to precipitation. *Water*
712 *Resources Research* 52(9):7086–7104
- 713 Hofstätter M, Lexer A, Homann M, Blöschl G (2018) Large-scale heavy precip-
714 itation over central europe and the role of atmospheric cyclone track types.
715 *International Journal of Climatology* 38:e497–e517
- 716 Imamovic A, Schlemmer L, Schär C (2019) Mountain volume control on deep-
717 convective rain amount during episodes of weak synoptic forcing. *Journal of*
718 *the Atmospheric Sciences* 76(2):605–626
- 719 James P, Stohl A, Spichtinger N, Eckhardt S, Forster C (2004) Climatological
720 aspects of the extreme european rainfall of august 2002 and a trajectory
721 method for estimating the associated evaporative source regions. *Natural*
722 *Hazards and Earth System Sciences* 4(5/6):733–746
- 723 Kelemen FD, Primo C, Feldmann H, Ahrens B (2019) Added value of
724 atmosphere-ocean coupling in a century-long regional climate simulation.
725 *Atmosphere* 10(9):537
- 726 Kinne S, Schulz M, Textor C, Guibert S, Balkanski Y, Bauer SE, Bernsten T,
727 Berglen T, Boucher O, Chin M, et al (2006) An aerocom initial assessment–
728 optical properties in aerosol component modules of global models. *Atmo-*
729 *spheric Chemistry and Physics* 6(7):1815–1834
- 730 Krug A, Aemisegger F, Sprenger M, Ahrens B (2021a) What intensifies vb-
731 cyclone precipitation in central europe? *Climate Dynamics*
- 732 Krug A, Pothapakula PK, Primo C, Ahrens B (2021b) Heavy vb-cyclone
733 precipitation: a transfer entropy application showcase. *Meteorologische*
734 *Zeitschrift*
- 735 Leduc M, Mailhot A, Frigon A, Martel JL, Ludwig R, Brietzke GB, Giguère
736 M, Brissette F, Turcotte R, Braun M, et al (2019) The climex project: a
737 50-member ensemble of climate change projections at 12-km resolution over
738 europe and northeastern north america with the canadian regional climate
739 model (crcom5). *Journal of Applied Meteorology and Climatology* 58(4):663–
740 693
- 741 Lizier JT (2014) Jidt: An information-theoretic toolkit for studying the dy-
742 namics of complex systems. *Frontiers in Robotics and AI* 1:11
- 743 Messmer M, Gómez-Navarro JJ, Raible CC (2015) Climatology of vb cyclones,
744 physical mechanisms and their impact on extreme precipitation over central
745 europe. *Earth system dynamics* 6(2):541–553
- 746 Messmer M, Gómez-Navarro JJ, Raible CC (2017) Sensitivity experiments on
747 the response of vb cyclones to sea surface temperature and soil moisture
748 changes. *Earth system dynamics* 8(3):477–493
- 749 Messmer M, Raible CC, Gómez-Navarro JJ (2020) Impact of climate change
750 on the climatology of vb cyclones. *Tellus A: Dynamic Meteorology and*
751 *Oceanography* 72(1):1–18

- 752 Mittermeier M, Braun M, Hofstätter M, Wang Y, Ludwig R (2019) Detecting
753 climate change effects on vb cyclones in a 50-member single-model ensemble
754 using machine learning. *Geophysical Research Letters* 46(24):14,653–14,661
- 755 Nishant N, Sherwood SC (2021) How strongly are mean and extreme precipi-
756 tation coupled? *Geophysical Research Letters* 48(10):e2020GL092,075
- 757 Nissen KM, Ulbrich U, Leckebusch GC (2013) Vb cyclones and associated
758 rainfall extremes over central europe under present day and climate change
759 conditions. *Meteorologische Zeitschrift* 22(6):649–660
- 760 Oki T, Sud Y (1998) Design of total runoff integrating pathways (trip)—a
761 global river channel network. *Earth interactions* 2(1):1–37
- 762 Panosetti D, Schlemmer L, Schär C (2019) Bulk and structural convergence
763 at convection-resolving scales in real-case simulations of summertime moist
764 convection over land. *Quarterly Journal of the Royal Meteorological Society*
765 145(721):1427–1443
- 766 Poli P, Hersbach H, Dee DP, Berrisford P, Simmons AJ, Vitart F, Laloyaux
767 P, Tan DG, Peubey C, Thépaut JN, et al (2016) Era-20c: An atmospheric
768 reanalysis of the twentieth century. *Journal of Climate* 29(11):4083–4097
- 769 Pothapakula PK, Primo C, Ahrens B (2019) Quantification of information
770 exchange in idealized and climate system applications. *Entropy* 21(11):1094
- 771 Pothapakula PK, Primo C, Sørland S, Ahrens B (2020) The synergistic im-
772 pact of enso and iod on indian summer monsoon rainfall in observations
773 and climate simulations—an information theory perspective. *Earth System*
774 *Dynamics* 11(4):903–923
- 775 Primo C, Kelemen FD, Feldmann H, Akhtar N, Ahrens B (2019) A regional
776 atmosphere–ocean climate system model (cclmv5. 0clm7-nemov3. 3-nemov3.
777 6) over europe including three marginal seas: on its stability and perfor-
778 mance. *Geoscientific Model Development* 12(12):5077–5095
- 779 Rayner N, Parker DE, Horton E, Folland CK, Alexander LV, Rowell D, Kent
780 EC, Kaplan A (2003) Global analyses of sea surface temperature, sea ice,
781 and night marine air temperature since the late nineteenth century. *Journal*
782 *of Geophysical Research: Atmospheres* 108(D14)
- 783 Reynolds RW, Rayner NA, Smith TM, Stokes DC, Wang W (2002) An im-
784 proved in situ and satellite sst analysis for climate. *Journal of climate*
785 15(13):1609–1625
- 786 Ritter B, Geleyn JF (1992) A comprehensive radiation scheme for numerical
787 weather prediction models with potential applications in climate simula-
788 tions. *Monthly weather review* 120(2):303–325
- 789 Rockel B, Geyer B (2008) The performance of the regional climate model cfm
790 in different climate regions, based on the example of precipitation. *Meteo-*
791 *rologische Zeitschrift* 17(4):487–498
- 792 Ruddell BL, Drewry DT, Nearing GS (2019) Information theory for model
793 diagnostics: Structural error is indicated by trade-off between functional
794 and predictive performance. *Water Resources Research* 55(8):6534–6554
- 795 Russo E, Sørland SL, Kirchner I, Schaap M, Raible CC, Cubasch U (2020)
796 Exploring the parameters space of the regional climate model cosmo-clm
797 5.0 for the cordex central asia domain. *Geoscientific Model Development*

- 798 Discussions 2020:1–33
- 799 Ruti PM, Somot S, Giorgi F, Dubois C, Flaounas E, Obermann A, Dell’Aquila
800 A, Pisacane G, Harzallah A, Lombardi E, et al (2016) Med-cordex initiative
801 for mediterranean climate studies. *Bulletin of the American Meteorological*
802 *Society* 97(7):1187–1208
- 803 Schlemmer L, Schär C, Lüthi D, Strebel L (2018) A groundwater and runoff
804 formulation for weather and climate models. *Journal of Advances in Mod-*
805 *eling Earth Systems* 10(8):1809–1832
- 806 Seneviratne S, Nicholls N, Easterling D, Goodess C, Kanae S, Kossin J, Luo Y,
807 Marengo J, McInnes K, Rahimi M, et al (2012) Changes in climate extremes
808 and their impacts on the natural physical environment
- 809 Sevault F, Somot S, Alias A, Dubois C, Lebeaupin-Brossier C, Nabat P, Adloff
810 F, Deque M, Decharme B (2014) A fully coupled mediterranean regional
811 climate system model: design and evaluation of the ocean component for
812 the 1980–2012 period. *Tellus A: Dynamic Meteorology and Oceanography*
813 66(1):23,967
- 814 Shannon CE (1948) A mathematical theory of communications. *Bell Syst Tech*
815 *J* 27:379–423
- 816 Sodemann H, Wernli H, Schwierz C (2009) Sources of water vapour con-
817 tributing to the elbe flood in august 2002—a tagging study in a mesoscale
818 model. *Quarterly Journal of the Royal Meteorological Society: A journal of*
819 *the atmospheric sciences, applied meteorology and physical oceanography*
820 135(638):205–223
- 821 Somot S, Sevault F, Déqué M, Crépon M (2008) 21st century climate change
822 scenario for the mediterranean using a coupled atmosphere–ocean regional
823 climate model. *Global and Planetary Change* 63(2-3):112–126
- 824 Sørland SL, Brogli R, Pothapakula PK, Russo E, Van de Walle J, Ahrens B,
825 Anders I, Bucchignani E, Davin EL, Demory ME, et al (2021) Cosmo-clm
826 regional climate simulations in the coordinated regional climate downscaling
827 experiment (cordex) framework: a review. *Geoscientific Model Development*
828 14(8):5125–5154
- 829 Soto-Navarro J, Jordá G, Amores A, Cabos W, Somot S, Sevault F, Macías D,
830 Djurdjevic V, Sannino G, Li L, et al (2020) Evolution of mediterranean sea
831 water properties under climate change scenarios in the med-cordex ensemble.
832 *Climate Dynamics* 54(3):2135–2165
- 833 Sprenger M, Fragkoulidis G, Binder H, Croci-Maspoli M, Graf P, Grams CM,
834 Knippertz P, Madonna E, Schemm S, Škerlak B, et al (2017) Global cli-
835 matologies of eulerian and lagrangian flow features based on era-interim.
836 *Bulletin of the American Meteorological Society* 98(8):1739–1748
- 837 Stocker T, Qin D, Plattner GK, Tignor M, Allen S, Boschung J, Nauels A,
838 Xia Y, Bex V, (eds) PM (2013) The physical science basis. contribution
839 of working group i to the fifth assessment report of the intergovernmental
840 panel on climate change
- 841 Trenberth KE (1999) Conceptual framework for changes of extremes of the
842 hydrological cycle with climate change. In: *Weather and climate extremes*,
843 Springer, pp 327–339

- 844 Valcke S (2013) The oasis3 coupler: A european climate modelling community
845 software. *Geoscientific Model Development* 6(2):373–388
- 846 Volosciuk C, Maraun D, Semenov VA, Tilinina N, Gulev SK, Latif M (2016)
847 Rising mediterranean sea surface temperatures amplify extreme summer
848 precipitation in central europe. *Scientific reports* 6(1):1–7
- 849 Wernli H, Schwierz C (2006) Surface cyclones in the era-40 dataset (1958–
850 2001). part i: Novel identification method and global climatology. *Journal*
851 *of the atmospheric sciences* 63(10):2486–2507
- 852 Wicker LJ, Skamarock WC (2002) Time-splitting methods for elastic models
853 using forward time schemes. *Monthly weather review* 130(8):2088–2097
- 854 Wilcox EM, Donner LJ (2007) The frequency of extreme rain events in satellite
855 rain-rate estimates and an atmospheric general circulation model. *Journal*
856 *of Climate* 20(1):53–69

Supplementary Files

This is a list of supplementary files associated with this preprint. Click to download.

- [Supplementary.pdf](#)